ELSEVIER

International Journal of Solids and Structures 41 (2004) 4137–4161

INTERNATIONAL JOURNAL OF SOLIDS and STRUCTURES

www.elsevier.com/locate/ijsolstr

Fracture analysis of cracked piezoelectric materials

Xian-Fang Li [a,b,*], Kang Yong Lee [c,*]

[a] *Institute of Mechanics and Sensor Technology, School of Civil Engineering and Architecture, Central South University, Changsha, Hunan 410083, PR China*

[b] *College of Mathematics and Computer Science, Hunan Normal University, Changsha, Hunan 410081, PR China*

[c] *School of Mechanical Engineering, Yonsei University, Seoul 120-749, South Korea*

Received 15 August 2003; received in revised form 17 February 2004

Available online 27 March 2004

Abstract

A piezoelectric material with a Griffith crack perpendicular to the poling axis is analyzed within the framework of the theory of linear piezoelectricity. Using exact electric boundary conditions at the crack surfaces, the nonlinear behavior between the electric displacement at the crack faces and applied loading is given, and it can be approximated by a linear relation on applied electric field. The Fourier transform technique is employed to reduce the mixed boundary value problem to dual integral equations. Solving resulting equations, expressions for the electroelastic field in the entire plane are obtained explicitly for a cracked piezoelectric material subjected to uniform combined electromechanical loading. The distribution of asymptotic field and the intensity factors of electroelastic field as well as the elastic T-stress are determined. Particularly, the maximum hoop strain $s_{\theta\theta}$ is suggested as a fracture criterion for piezoelectric materials. Based on this criterion, relevant experimental results can be explained successfully. As an illustrative example, theoretical predictions for PZT-4 ceramic with a crack are in excellent agreement with existing experimental data, not only in qualitative behavior but also in quantitative results.

Keywords: Fracture criterion; Crack; Complete solution; Piezoelectric materials; Maximum hoop strain; Fourier transform

1. Introduction

Piezoelectric/ferroelectric ceramics have been used widely in techniques such as actuators, sensors, transducers, etc. due to the intrinsic coupling feature between elastic and electric behaviors (Rao and Sunar, 1994). However, a main disadvantage is that they are very susceptible to fracture because of their brittleness. Owing to various causes, cracks or flaws are inevitably present in these materials, which gives rise to electroelastic field concentration under applied electromechanical loading, rising high enough to cause the crack advance, and finally leads to serious degradation of the performance of piezoelectric materials (Pisarenko et al., 1985; Tobin and Pak, 1993; etc.). To understand the failure mechanism of piezoelectric materials and maintain the stability of cracked piezoelectric structures operating in an environment of

* Corresponding authors. Tel.: +86-73-1887-2667 (X.-F. Li), tel./fax: +82-2-2123-2813 (K.Y. Lee).

E-mail addresses: xfli00@china.com.cn (X.-F. Li), kyl2813@yahoo.co.kr (K.Y. Lee).

0020-7683/$ - see front matter © 2004 Elsevier Ltd. All rights reserved.

doi:10.1016/j.ijsolstr.2004.02.060

combined electromechanical loading, the analysis of elastic and electric behaviors is prerequisite. So far, great efforts in theory have been made on this field (e.g. Suo et al., 1992; Pak, 1990, 1992; Sosa, 1992; Dunn, 1994; Sosa and Khutoryansky, 1996; Zhang et al., 1998, Ru, 1999; Gao and Fan, 1999; Shindo et al., 2000; McMeeking, 2001; Xu and Rajapakse, 2001; Liu and Hsia, 2003; etc.) In particular, a significant matter is to establish fracture criterion applicable to piezoelectric materials.

As we know, within the framework of the theory of linear elastic fracture mechanics there exist many fracture criteria for a purely elastic medium, and these criteria mainly contain those of stress intensity factor, energy release rate (or J-integral, crack driving force), energy density factor, etc. However, the above-mentioned these criteria for a purely elastic medium seem unlikely to generalize directly to piezoelectric materials due to the introduction of electric field along with the coupling of electric and elastic fields. For example, the stress intensity factor criterion is clearly unsuitable for a cracked piezoelectric material, since stress intensity factors near a crack tip are independent of applied electric loading provided that applied stress is prescribed regardless of an impermeable crack (Pak, 1992; Sosa, 1992) or a permeable crack (Sosa and Khutoryansky, 1996; Zhang et al., 1998; Gao and Fan, 1999; Shindo et al., 2000). It implies that crack growth depends only upon applied mechanical stress, not upon electric loading, which is inconsistency with the experimental observations that a positive electric field promotes crack growth and a negative one impedes crack growth.

On the other hand, based on the energy release rate criterion, it is readily shown that the total energy release rate G is composed of two parts, $G = G^{\mathrm{m}} + G^{\mathrm{e}}$, one corresponding to the mechanical part G^{m} and the other to the electric part G^{e}. Moreover, $G^{\mathrm{e}} = 0$ for a permeable crack, leading to applied electric fields have no influence on crack advance, which is clearly unreasonable, while $G^{\mathrm{e}} < 0$ for an impermeable crack under positive and negative electric fields, indicating that applied electric fields always hinder crack propagation irrespective of their directions, which is contradictory to the experimental results. To amend this drawback, some modified models have been proposed. Gao et al. (1997) and Fulton and Gao (2001) adopted a multiscale viewpoint, assumed electric nonlinearity ahead of the crack tip and proposed a local energy release rate as a fracture criterion accounting for crack propagation.

Based on the fact that crack growth is a process of mechanical deformation, Park and Sun (1995) formulated mechanical strain energy release rate as a fracture criterion of piezoelectric materials, and revealed that the theoretical prediction is in accordance with their experimental data. However, since the released mechanical energy, not the total energy, was only considered during crack growth, the effect of G^{e} on crack growth is dropped. Similarly, adopting small scale electric saturation in front of the crack tip (Gao et al., 1997), Fang et al. (1999) evaluated the energy release rate and found that $G^{\mathrm{e}} = 0$ in this case, leading to that G is identical to G^{m}. Recently, the analysis by Guiu et al. (2003) also indicates that the energy release rate or crack extension force is, indeed, not suitable parameter for piezoelectric materials, and that the rate of mechanical work is an acceptable criterion. Now, a clear understanding of the roles of G^{e} in the fracture of piezoelectric materials is still lacking. In particular, for cracked dielectrics G^{e} is introduced in analogy with energy release rate in linear elastic fracture mechanics and used to characterize breakdown of electric behavior in dielectrics (Garboczi, 1988; Ouyang and Lee, 1998). In other words, G^{e} affects only electric breakdown and does not affect crack (mechanical) growth. According to this viewpoint, the role of G^{e} in piezoelectric materials can account for electric breakdown of piezoelectric materials and only G^{m} affects mechanical failure of piezoelectric materials. Further, in theory if imposing all the piezoelectric constants vanish, meaning that a piezoelectric material reduces to an elastic dielectric without coupling between mechanical deformation and electric field, the influence of electric field, of course, is independent of crack growth. Nevertheless, under such circumstances, the total energy release rate G is still composed of G^{m} and G^{e}, and the contribution of G^{e} on crack propagation is visible, which is clearly contrary to practical situation.

Furthermore, crack growth driven by purely electric fields in poled ferroelectrics has been observed in experiment (Cao and Evans, 1994; Schneider and Heyer, 1999; Shang and Tan, 2001; dos Santos e Lucato

et al., 2002; etc.). Within the framework of linear piezoelectricity, G^{m} fails to predict crack advance in the absence of mechanical loading, since in this case $G^{\mathrm{m}} = 0$. Hence, Hwang et al. (1995), and Yang and Zhu (1998) proposed domain switching zone around the crack tip responsible for the anisotropy of fracture toughness induced by electric fields.

In this paper, fracture analysis of cracked piezoelectric materials is made, and maximum hoop strain (MHS) is suggested as a fracture criterion of piezoelectric materials. This paper is organized as follows. In Section 2, basic theory as well as exact natural electric boundary conditions at the crack surfaces are given. Section 3 is devoted to determining the complete electroelastic field of a piezoelectric material containing a crack perpendicular to the poling axis, by using the Fourier transform technique and solving dual integral equations. Meanwhile, the nonlinear behavior of electric displacement at the crack surfaces is determined. In Section 4, the crack tip asymptotic fields are obtained. Further the field intensity factors are determined, and the MHS criterion is presented. As an example, in Section 5 a PZT-4 ceramic containing a crack is considered. A comparison of theoretical predictions with existing experimental results is made, inferring the effectiveness of the MHS criterion for piezoelectric materials.

2. Statement of the problem

2.1. Basic equations

Consider an infinite transversely isotropic piezoelectric body with the poling axis as the z-axis and the isotropic plane as the xy-plane. With the framework of the theory of linear piezoelectricity, the constitutive equations restricted to the xoz-plane take the form

$$\sigma_{xx} = c_{11}s_{xx} + c_{13}s_{zz} - e_{31}E_z, \tag{1a}$$

$$\sigma_{zz} = c_{13}s_{xx} + c_{33}s_{zz} - e_{33}E_z, \tag{1b}$$

$$\sigma_{xz} = 2c_{44}s_{zx} - e_{15}E_x, \tag{1c}$$

$$D_x = 2e_{15}s_{zx} + \varepsilon_{11}E_x, \tag{1d}$$

$$D_z = e_{31}s_{xx} + e_{33}s_{zz} + \varepsilon_{33}E_z, \tag{1e}$$

where c_{ij}, ε_{ij}, and e_{ij} are the elastic stiffnesses, the dielectric permittivities, the piezoelectric constants, respectively. Here the components of strain and electric field can be expressed in terms of elastic displacements, $u_x(x,z)$, $u_z(x,z)$, and electric potential, $\phi(x,z)$, by the following equations, respectively:

$$s_{ij} = \frac{1}{2}(u_{i,j} + u_{j,i}), \qquad E_i = -\phi_{,i} \tag{2}$$

in which i, j stand for x and z.

In the absence of body forces and free charges, it follows from the equilibrium equations of stresses and electric displacements that elastic displacements and potential satisfy the basic governing equations

$$c_{11}u_{x,xx} + c_{44}u_{x,zz} + (c_{13} + c_{44})u_{z,xz} + (e_{31} + e_{15})\phi_{,xz} = 0, \tag{3a}$$

$$c_{44}u_{z,xx} + c_{33}u_{z,zz} + (c_{13} + c_{44})u_{x,xz} + e_{15}\phi_{,xx} + e_{33}\phi_{,zz} = 0, \tag{3b}$$

$$e_{15}u_{z,xx} + e_{33}u_{z,zz} + (e_{31} + e_{15})u_{x,xz} - \varepsilon_{11}\phi_{,xx} - \varepsilon_{33}\phi_{,zz} = 0. \tag{3c}$$

2.2. Boundary conditions

In what follows special attention is focused on a through Griffith crack of length $2a$ perpendicular to the poling axis, as shown in Fig. 1. In order to obtain a desired electroelastic field of a piezoelectric medium with a Griffith crack, appropriate boundary conditions must be furnished. First of all, for the elastic boundary conditions, the crack surfaces are free of stress, which can be written as

$$\sigma_{zz}(x,0)=0, \quad \sigma_{xz}(x,0)=0, \qquad |x|<a. \tag{4}$$

In addition, for electric boundary conditions at the crack surfaces, we adopt exact natural boundary conditions

$$D_n^{(\mathrm{p})}|_{\Gamma}=D_n^{(\mathrm{c})}|_{\Gamma}, \qquad E_t^{(\mathrm{p})}|_{\Gamma}=E_t^{(\mathrm{c})}|_{\Gamma}, \tag{5}$$

where n and t represent respectively the directions of the outward normal and tangential vectors of Γ, Γ being the boundary of crack posterior to deformation, not prior to deformation, a quantity with the superscripts (p) or (c) designates the one in the piezoelectric matrix or in the hole inside the opening crack, respectively, and the superscript (p) is commonly omitted without confusion.

In previous study involving crack problems of piezoelectric materials, electric boundary conditions of two types at the crack surfaces prevail. One is an impermeable crack, assuming that the electric displacement at the crack surfaces and inside the crack vanishes, and the other is a permeable crack, assuming that electric displacement and electric potential are continuous across the crack. However, a real crack is a dielectric with permittivity $\varepsilon^{(\mathrm{c})}$ $(=\varepsilon_r\varepsilon_0,\ \varepsilon_0=8.85\times10^{-12}$ F/m), $\varepsilon_r=1$ corresponding to an ideal vacuum crack. An impermeable crack simply enforces the requirement of $\varepsilon_r=0$, while a permeable crack ignores the contribution of the dielectric interior to crack on electroelastic field, both of which may give rise to an error. Here it is emphasized that the relations in (5) are assumed to be valid at the boundary of a deformed crack, which is contrast to the analysis by Shindo et al. (1997) for anti-plane shear crack and Yang (2001) for an in-plane mode-I crack, who applied (5) at the boundary of an undeformed crack, i.e. Γ in this case reduces to a mathematical cut having no thickness, $-a<x<a$, $y=0$. In effect, for the latter case, the problem can be easily shown to be identical to that under the electrically permeable assumption at the crack surfaces. According to the finite element analysis of McMeeking (1999), it is more reasonable and suitable to take Γ as the boundary of the opening crack in treating crack problems of piezoelectric materials. Moreover, recent experimental evidence (Schneider et al., 2003) revealed a distinct drop of electric potential between two surfaces of an opening crack, which implies the existence of electric field in the opening crack interior. Accordingly, the electric displacement vector $D^{(\mathrm{c})}$ inside the opening crack obeys

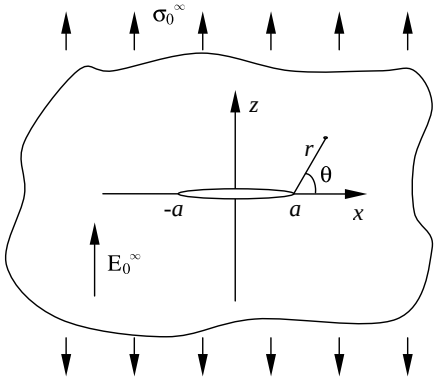

Fig. 1. Geometry of a piezoelectric material with a Griffith crack along with the corresponding coordinates.

$$D_x^{(c)} = \varepsilon^{(c)} E_x^{(c)}, \qquad D_z^{(c)} = \varepsilon^{(c)} E_z^{(c)}, \tag{6}$$

where $\varepsilon^{(c)} = \varepsilon_r \varepsilon_0$ is the dielectric permittivity of the crack interior, $\varepsilon_r = 1$ for a vacuum crack. The fact that the crack opening displacement is small as compared to the crack length allows us to further assume that $E_z^{(c)} = E_n^{(c)}|_\Gamma$, which may be supposed to be a constant, given by

$$E_z^{(c)} = -\frac{\Delta\phi}{\Delta u_z}, \tag{7}$$

where Δu_z and $\Delta\phi$ are the jumps of elastic displacement and potential across the crack. Furthermore, making use of (6) the electric displacement inside the opening crack is governed by the following relations:

$$D_z^{(c)} = -\varepsilon^{(c)} \frac{\Delta\phi}{\Delta u_z}, \tag{8}$$

which has also been used in dealing with certain crack problems such as Hao and Shen (1994), McMeeking (2001), Liu et al. (2001), Xu and Rajapakse (2001), Wang and Jiang (2002), and Wang and Mai (2003). It is interesting to note that impermeable and conducting cracks can be treated as the limiting cases of dielectric cracks as $\varepsilon^{(c)} \to 0$ and $\varepsilon^{(c)} \to \infty$, respectively.

For a Griffith crack embedded in an infinite piezoelectric body subjected to a uniform mechanical tension σ_0^∞ and constant electric field E_0^∞ at infinity (see Fig. 1), remote mechanical and electric boundary conditions can be written respectively below:

$$\sigma_{zz}(x,z) \to \sigma_0^\infty, \quad E_z(x,z) \to E_0^\infty, \qquad z \to \infty, \tag{9a}$$

$$\sigma_{xx}(x,z) \to 0, \quad E_x(x,z) \to 0, \qquad x \to \infty \tag{9b}$$

$$\sigma_{xz}(x,z) \to 0, \quad \sqrt{x^2+z^2} \to \infty. \tag{9c}$$

In general, it is easy to measure and control the electric field strength, rather than the electric displacement, in experiment. As a result, for electric boundary conditions, E_0^∞ is supposed to be prescribed. Of course, the case when electric displacement is given at infinity can be solved in a similar manner, which is omitted here. Here, applied electric fields parallel or anti-parallel to the poling axis are referred as to positive or negative electric fields, respectively.

3. Solution of the problem

In this section, we consider a Griffith crack of length $2a$ lying at a plane perpendicular to the poling direction. Obviously, it is sufficient to consider the upper half piezoelectric body. The electroelastic field in the lower part can be directly given by symmetry from the counterpart in the upper part. Hence in what follows we confine our attention to the upper half-plane.

3.1. General solution in terms of the Fourier integral

To solve the stated-above problem, following the analysis of Rajapakse (1997), we represent u_x, u_z and ϕ in terms of three generalized harmonic functions $F_j(x,z)$ which are governed by

$$F_{,zz} + \gamma^2 F_{,xx} = 0, \tag{10}$$

where γ^2 are three roots of the following characteristic equation:

$$a_0\gamma^6 + b_0\gamma^4 + c_0\gamma^2 + d_0 = 0, \tag{11}$$

where the constants a_0, b_0, c_0, and d_0 are given in Appendix A.

Consider a particular case of three distinct eigenvalues γ_j^2 ($j = 1, 2, 3$), and other cases are similar, which are omitted here for saving space. Further, if representing $F_j(x,z)$ by Fourier cosine integrals

$$F_j(x,z) = -\int_0^\infty \frac{1}{\xi} A_j(\xi)\, \mathrm{e}^{-\gamma_j \xi z} \cos(\xi x)\, \mathrm{d}\xi, \tag{12}$$

for $z \geqslant 0$, where $A_j(\xi)$'s are unknown functions to be determined through appropriate electric and elastic boundary conditions, and $\mathrm{Re}(\gamma_j)$ is chosen larger than zero to guarantee that the first and second derivatives of $F_j(x,z)$ with respect to x and z vanish at infinity, we can then get a general formal solution suitable for dealing with the problem posed by (9), in terms of $A_j(\xi)$ as follows:

$$u_x(x,z) = \sum_{j=1}^{3} \int_0^\infty A_j(\xi)\, \mathrm{e}^{-\gamma_j \xi z} \sin(\xi x)\, \mathrm{d}\xi + B_1 x, \tag{13a}$$

$$u_z(x,z) = \sum_{j=1}^{3} \eta_{3j}\gamma_j \int_0^\infty A_j(\xi)\, \mathrm{e}^{-\gamma_j \xi z} \cos(\xi x)\, \mathrm{d}\xi + B_3 z, \tag{13b}$$

$$\phi(x,z) = \sum_{j=1}^{3} \eta_{4j}\gamma_j \int_0^\infty A_j(\xi)\, \mathrm{e}^{-\gamma_j \xi z} \cos(\xi x)\, \mathrm{d}\xi + B_4 z, \tag{13c}$$

where B_k ($k = 1, 3, 4$) are unknown constants to be determined, and η_{3j} and η_{4j} are constants which are determined by the following relations:

$$\frac{c_{11}}{c_{44} + (c_{13} + c_{44})\eta_{3j} + (e_{31} + e_{15})\eta_{4j}} = \frac{c_{13} + c_{44} + c_{44}\eta_{3j} + e_{15}\eta_{4j}}{c_{33}\eta_{3j} + e_{33}\eta_{4j}} = \frac{e_{31} + e_{15} + e_{15}\eta_{3j} - \varepsilon_{11}\eta_{4j}}{e_{33}\eta_{3j} - \varepsilon_{33}\eta_{4j}} = \gamma_j^2. \tag{14}$$

Moreover, from the constitutive equations, expressions for the stresses and electric displacements in terms of $A_j(\xi)$ are also obtainable. They are

$$\sigma_{xx}(x,z) = -\sum_{j=1}^{3} \beta_{0j} \int_0^\infty \xi A_j(\xi)\, \mathrm{e}^{-\gamma_j \xi z} \cos(\xi x)\, \mathrm{d}\xi + c_{11}B_1 + c_{13}B_3 + e_{31}B_4, \tag{15a}$$

$$\sigma_{zz}(x,z) = -\sum_{j=1}^{3} \beta_{1j} \int_0^\infty \xi A_j(\xi)\, \mathrm{e}^{-\gamma_j \xi z} \cos(\xi x)\, \mathrm{d}\xi + c_{13}B_1 + c_{33}B_3 + e_{33}B_4, \tag{15b}$$

$$\sigma_{xz}(x,z) = -\sum_{j=1}^{3} \beta_{2j} \int_0^\infty \xi A_j(\xi)\, \mathrm{e}^{-\gamma_j \xi z} \sin(\xi x)\, \mathrm{d}\xi, \tag{15c}$$

$$D_x(x,z) = -\sum_{j=1}^{3} \beta_{3j} \int_0^\infty \xi A_j(\xi)\, \mathrm{e}^{-\gamma_j \xi z} \sin(\xi x)\, \mathrm{d}\xi, \tag{15d}$$

$$D_z(x,z) = -\sum_{j=1}^{3} \beta_{4j} \int_0^\infty \xi A_j(\xi)\, \mathrm{e}^{-\gamma_j \xi z} \cos(\xi x)\, \mathrm{d}\xi + e_{31}B_1 + e_{33}B_3 - \varepsilon_{33}B_4, \tag{15e}$$

where

$$\beta_{0j} = (c_{13}\eta_{3j} + e_{31}\eta_{4j})\gamma_j^2 - c_{11}, \tag{16a}$$

$$\beta_{1j} = (c_{33}\eta_{3j} + e_{33}\eta_{4j})\gamma_j^2 - c_{13}, \tag{16b}$$

$$\beta_{2j} = [c_{44}(1 + \eta_{3j}) + e_{15}\eta_{4j}]\gamma_j, \tag{16c}$$

$$\beta_{3j} = [e_{15}(1 + \eta_{3j}) - \varepsilon_{11}\eta_{4j}]\gamma_j, \tag{16d}$$

$$\beta_{4j} = (e_{33}\eta_{3j} - \varepsilon_{33}\eta_{4j})\gamma_j^2 - e_{31}. \tag{16e}$$

As a straightforward check, substitution of (15) into the equilibrium equations reveals that them are satisfied identically. The remaining task is how to get unknown B_j and $A_j(\xi)$ through appropriate electric and elastic boundary conditions and further determine electroelastic field for the corresponding crack problem.

3.2. Derivation of dual integral equations

Consideration of symmetry of the problem allows us to conclude that the shear stress at the crack plane vanishes, i.e.

$$\sigma_{xz}(x, 0) = 0, \quad -\infty < x < \infty. \tag{17a}$$

Since attention is restricted to the upper half-plane, the following condition:

$$u_z(x, 0) = 0, \quad \phi(x, 0) = 0, \qquad |x| \geqslant a \tag{17b}$$

must be supplemented because of symmetry of the problem. Besides, at the crack surfaces, electromechanical boundary conditions

$$\sigma_{zz}(x, 0) = 0, \quad -a < x < a, \tag{17c}$$

$$D_z(x, 0) = D^{(c)}, \quad -a < x < a, \tag{17d}$$

where $D^{(c)}$ is a parameter to be determined, governed by the relation (8).

Firstly, to look for three unknown constants B_k ($k = 1, 3, 4$) involved in (15), application of the boundary conditions at infinity in (9) results readily in a system of linear equations, which can be used to determine uniquely B_k ($k = 1, 3, 4$). The final result is given in Appendix A. Knowledge of B_k ($k = 1, 3, 4$) permits us to further seek the disturbed electroelastic field of a piezoelectric body weakened by a Griffith crack. To this end, by substituting the above results into (13) and (15), utilizing the boundary conditions (17a) yields

$$\sum_{j=1}^{3} \beta_{2j} A_j(\xi) = 0. \tag{18}$$

Also, application of (15b) and (15e) to the conditions (17c) and (17d), respectively, leads to

$$-\sum_{j=1}^{3} \beta_{1j} \int_0^\infty \xi A_j(\xi) \cos(\xi x)\, \mathrm{d}\xi + \sigma_0^\infty = 0, \quad -a < x < a, \tag{19a}$$

$$-\sum_{j=1}^{3} \beta_{4j} \int_0^\infty \xi A_j(\xi) \cos(\xi x)\, \mathrm{d}\xi + D_z^\infty = D^{(c)}, \quad -a < x < a, \tag{19b}$$

with

$$D^{(c)} = -\varepsilon^{(c)} \frac{\sum_{j=1}^{3} \eta_{4j}\gamma_j \int_0^\infty A_j(\xi)\cos(\xi x)\,\mathrm{d}\xi}{\sum_{j=1}^{3} \eta_{3j}\gamma_j \int_0^\infty A_j(\xi)\cos(\xi x)\,\mathrm{d}\xi}, \quad -a < x < a, \tag{20a}$$

$$D_z^\infty = \frac{c_{11}e_{33} - c_{13}e_{31}}{c_{11}c_{33} - c_{13}^2}\sigma_0^\infty + \left[\frac{c_{33}e_{31}^2 + c_{11}e_{33}^2 - 2c_{13}e_{33}e_{31}}{c_{11}c_{33} - c_{13}^2} + \varepsilon_{33}\right]E_0^\infty. \tag{20b}$$

Additionally, from (13b) and (13c) in conjunction with the conditions in (17b) we have

$$\sum_{j=1}^{3} \eta_{3j}\gamma_j \int_0^\infty A_j(\xi)\cos(\xi x)\,\mathrm{d}\xi = 0, \quad |x| \geqslant a, \tag{21a}$$

$$\sum_{j=1}^{3} \eta_{4j}\gamma_j \int_0^\infty A_j(\xi)\cos(\xi x)\,\mathrm{d}\xi = 0, \quad |x| \geqslant a. \tag{21b}$$

Thus we obtain coupled system of dual integral equations for $A_j(\xi)$ $(j = 1, 2, 3)$ with a parameter $D^{(c)}$ governed by (20a). In the following, we first determine the electric displacement $D^{(c)}$ at the crack surfaces, and then solve dual integral equations.

3.3. Electric displacement at the crack surfaces

In the resulting dual integral equations, an undetermined electric displacement $D^{(c)}$ is involved. In this subsection, we shall give an explicit analytic expression for calculating $D^{(c)}$ and a simple form of approximating $D^{(c)}$. Since $D^{(c)}$ is clearly independent of ξ, it immediately follows from (20a) that

$$\int_0^\infty \sum_{j=1}^{3} \left[D^{(c)}\eta_{3j} + \varepsilon^{(c)}\eta_{4j}\right]\gamma_j A_j(\xi)\cos(\xi x)\,\mathrm{d}\xi = 0, \quad -a < x < a, \tag{22}$$

which, together with (21), gives

$$\sum_{j=1}^{3} \left[D^{(c)}\eta_{3j} + \varepsilon^{(c)}\eta_{4j}\right]\gamma_j A_j(\xi) = 0. \tag{23}$$

Now we arrive at two Eqs. (18) and (23) for $A_j(\xi)$ $(j = 1, 2, 3)$, which are solvable up to two unknowns. In other words, two unknowns may be represented by the remaining one. To achieve this, we may choose a new intermediate auxiliary function $A(\xi)$ such that

$$A_j(\xi) = a_j A(\xi), \tag{24}$$

where a_j's are constants. Putting the above into (18) and (23) yields, respectively,

$$\sum_{j=1}^{3} \beta_{2j}a_j = 0, \tag{25a}$$

$$\sum_{j=1}^{3} \left[D^{(c)}\eta_{3j} + \varepsilon^{(c)}\eta_{4j}\right]\gamma_j a_j = 0. \tag{25b}$$

Furthermore, substituting (24) into (19a) and (19b), a comparison results in

$$\sigma_0^\infty \sum_{j=1}^{3} \beta_{4j} a_j + \left[D^{(c)} - D_z^\infty\right] \sum_{j=1}^{3} \beta_{1j} a_j = 0. \tag{25c}$$

Accordingly, Eqs. (25a), (25b) and (25c) form a system of linear algebraic equations for a_j, which can be rewritten in a compact form

$$\Lambda \begin{bmatrix} a_1 \\ a_2 \\ a_3 \end{bmatrix} = \begin{bmatrix} 0 \\ 0 \\ 0 \end{bmatrix}, \tag{26}$$

with

$$\Lambda = \begin{bmatrix} \beta_{11}\left[D^{(c)} - D_z^\infty\right] + \beta_{41}\sigma_0^\infty & \beta_{12}\left[D^{(c)} - D_z^\infty\right] + \beta_{42}\sigma_0^\infty & \beta_{13}\left[D^{(c)} - D_z^\infty\right] + \beta_{43}\sigma_0^\infty \\ \beta_{21} & \beta_{22} & \beta_{23} \\ \left[\eta_{31}D^{(c)} + \eta_{41}\varepsilon^{(c)}\right]\gamma_1 & \left[\eta_{32}D^{(c)} + \eta_{42}\varepsilon^{(c)}\right]\gamma_2 & \left[\eta_{33}D^{(c)} + \eta_{43}\varepsilon^{(c)}\right]\gamma_3 \end{bmatrix}. \tag{27}$$

In order to obtain a nontrivial solution of this equation, the determinant of the matrix Λ must take zero, i.e.

$$\det(\Lambda) = 0. \tag{28}$$

Expanding this determinant yields a quadric equation for $D^{(c)}$. In particular, for several special situations, $D^{(c)}$ may be determined via some simple expressions.

(I) In the absence of applied mechanical loading at infinity, this situation gives

$$D^{(c)} = D_z^\infty \quad \text{or} \quad D^{(c)} = -\frac{\det[\beta_1, \beta_2, \eta_2]}{\det[\beta_1, \beta_2, \eta_1]}\varepsilon^{(c)}. \tag{29}$$

Hereafter β_k denotes the vector composed of $(\beta_{k1}, \beta_{k2}, \beta_{k3})^{\mathrm{T}}$ $(k = 0, 1, \ldots, 4)$, and η_{k-2} denotes the vector composed of $(\eta_{k1}\gamma_1, \eta_{k2}\gamma_2, \eta_{k3}\gamma_3)^{\mathrm{T}}$ $(k = 3, 4)$, T being the transposition. Obviously, the first solution pertains to the case where a piezoelectric body without crack or two crack surfaces contact each other, and the second solution is reliant on the material properties and not on applied loading suitable for an opening crack. From this, one further finds electric field inside the opening crack to be a constant $-\det[\beta_1, \beta_2, \eta_2]/\det[\beta_1, \beta_2, \eta_1]$, independent of applied electric field and the dielectric permittivity.

(II) In the case of an impermeable crack, $\varepsilon^{(c)}$ is approximately assumed to be zero. Here, from the obtained solution we find

$$D^{(c)} = 0 \quad \text{or} \quad D^{(c)} = D_z^\infty - \sigma_0^\infty \frac{\det[\beta_4, \beta_2, \eta_1]}{\det[\beta_1, \beta_2, \eta_1]}. \tag{30}$$

Clearly, from the physical interpretation, the former $D^{(c)} = 0$ is suitable only for an opening crack and the other solution for a closed crack.

(III) For a conducting crack, $\varepsilon^{(c)}$ is commonly set to be infinity. In this situation, we obtain

$$D^{(c)} = D_z^\infty - \sigma_0^\infty \frac{\det[\beta_4, \beta_2, \eta_2]}{\det[\beta_1, \beta_2, \eta_2]}, \tag{31}$$

which indicates that $D^{(c)}$ is a linear function of applied electric loading as well as applied mechanical loading.

In general, Eq. (28) admits two roots for a dielectric crack, expressed as

$$D^{(c)} = \frac{-m_1 \pm \sqrt{m_1^2 - 4m_0m_2}}{2m_2}, \tag{32}$$

where m_0, m_1, and m_2 are given in Appendix A. And only one is reasonable and the other is superfluous, which should be neglected. Since ε_r is finite and lies in a range of 0 to ∞, corresponding to an impermeable and conducting cracks, respectively, the corresponding electric displacement $D^{(c)}$ inside the opening crack should be located at the range between two limiting values corresponding to $\varepsilon_r = 0$ and 1, respectively. Thus, an acceptable $D^{(c)}$ may be selected. An alternative approach for determining an acceptable $D^{(c)}$ is to look for the one such that $\Delta u_z(x,0) \geqslant 0$, the physical interpretation of which is obviously to avoid penetration of two crack surfaces. By computing for many practical examples, we find that, $D^{(c)}$ selected from the above-mentioned two methods are identical. This result indicates that apart from the material properties of the piezoelectric matrix, the electric displacement $D^{(c)}$ of the crack interior is also dependent on the dielectric permittivity of the crack interior. Moreover, not only applied electric loading but also on applied mechanical loading at infinity have pronounced influence on $D^{(c)}$. The dependence of $D^{(c)}$ on E_0^∞ for various dielectric permittivity of the crack interior in a PZT-4 ceramic with a crack is shown in Fig. 2, from which it is seen for a dielectric crack, the electric displacement at the crack surfaces is close to that for a conducting crack, and far away from that for an impermeable crack. Especially, it is interesting to note that $D^{(c)}$ does not vanish as E_0^∞ is less than about -8.2 kV/cm in Fig. 2, inferring that at this stage the crack does not open and $D^{(c)}$ is therefore determined by the second in (30). Further, due to the complexity of dependence (32) of $D^{(c)}$ on $\varepsilon^{(c)}$ (or ε_r) and applied loading, we present an approximate linear relation between $D^{(c)}$ and applied electric fields for computing $D^{(c)}$ by the following form:

$$D_{ap}^{(c)} = \lambda_E E_0^\infty, \tag{33}$$

with

$$\lambda_E = \frac{\varepsilon^{(c)} g_2 \det[\beta_1, \beta_2, \eta_2]}{\varepsilon^{(c)} \det[\beta_1, \beta_2, \eta_2] + \sigma_0^\infty \det[\beta_4, \beta_2, \eta_1] - g_1 \sigma_0^\infty \det[\beta_1, \beta_2, \eta_1]}, \tag{34a}$$

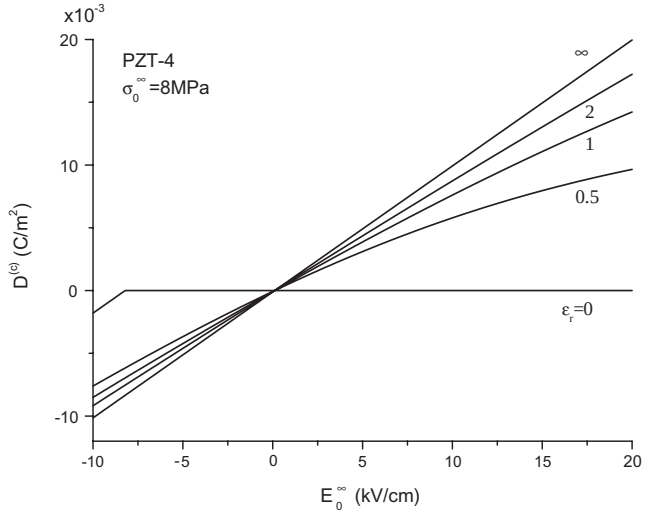

Fig. 2. Electric displacement at the crack surfaces versus applied electric field with $\sigma_0^\infty = 8$ MPa for various values of ε_r for a PZT-4 ceramic.

Table 1
The relevant material properties

	Elastic stiffnesses ($\times 10^{10}$ N/m^2)					Piezoelectric constants (C/m^2)			Dielectric permittivities ($\times 10^{-10}$ F/m)	
	c_{11}	c_{33}	c_{44}	c_{12}	c_{13}	e_{31}	e_{33}	e_{15}	ε_{11}	ε_{33}
PZT-4	13.9	11.3	2.56	7.78	7.43	−6.98	13.84	13.44	60	54.7

where

$$g_1 = \frac{c_{11}e_{33} - c_{13}e_{31}}{c_{11}c_{33} - c_{13}^2}, \qquad g_2 = \frac{c_{33}e_{31}^2 + c_{11}e_{33}^2 - 2c_{13}e_{33}e_{31}}{c_{11}c_{33} - c_{13}^2}, \tag{34b}$$

which is very accurate for E_0^∞ taking in a range from −10 to 10 kV/cm. For example, for a PZT-4 ceramic with relevant material properties listed in Table 1, the exact and approximate electric displacements, $D^{(c)}$ and $D_{ap}^{(c)}$, at the vacuum crack surfaces are very close for $\sigma_0^\infty = 5$ and 20 MPa, which is displayed in Fig. 3.

3.4. Full electroelastic field in the entire piezoelectric plane

Once $D^{(c)}$ is determined, nontrivial solution a_j can be expressed in terms of $D^{(c)}$ via solving equations arbitrary two equations among (25a), (25b) and (25c). For example, solving (25a) and (25c) we obtain

$$\begin{bmatrix} a_2/a_1 \\ a_3/a_1 \end{bmatrix} = -\begin{bmatrix} \beta_{22} & \beta_{23} \\ \sigma_0^\infty\beta_{42} + \left[D^{(c)} - D_z^\infty\right]\beta_{12} & \sigma_0^\infty\beta_{43} + \left[D^{(c)} - D_z^\infty\right]\beta_{13} \end{bmatrix}^{-1} \times \begin{bmatrix} \beta_{21} \\ \sigma_0^\infty\beta_{41} + \left[D^{(c)} - D_z^\infty\right]\beta_{11} \end{bmatrix}. \tag{35}$$

Next, applying the boundary conditions (19a) and (21a) we get a pair of simultaneous dual integral equations for $A(\xi)$

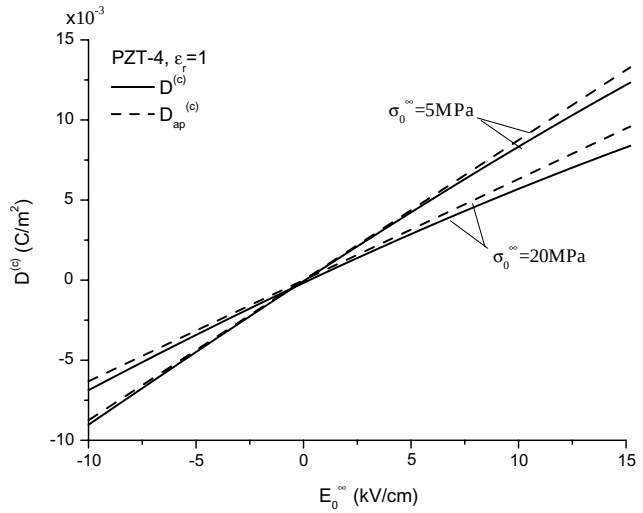

Fig. 3. Comparison of exact and approximate electric displacements at the crack surfaces for a vacuum crack under $\sigma_0^\infty = 5$ and 20 MPa.

$$\int_0^\infty \xi A(\xi)\cos(\xi x)\,\mathrm{d}\xi = \frac{\sigma_0^\infty}{\kappa_m}, \quad |x| < a, \tag{36a}$$

$$\int_0^\infty A(\xi)\cos(\xi x)\,\mathrm{d}\xi = 0, \quad |x| \geqslant a, \tag{36b}$$

where

$$\kappa_m = \sum_{j=1}^{3} \beta_{1j} a_j. \tag{37}$$

Hence, employing standard theory of dual integral equations, a solution of the above equations is readily found to be

$$A(\xi) = \frac{aJ_1(\xi a)}{\xi}\,\frac{\sigma_0^\infty}{\kappa_m}, \tag{38}$$

where $J_1(\cdot)$ is the first-order Bessel function of the first kind.

It is pointed out that the above result is only suitable for the case where applied mechanical loading at infinity is nonzero, i.e. $\sigma_0^\infty \neq 0$. Evidently, in the absence of mechanical loading, in view of the coupling characteristic, applied electric loading also causes deformation of a piezoelectric body and further may give rise to crack opening. However, in the case of $\sigma_0^\infty = 0$ the above result gives $A(\xi) = 0$, which fails to cause crack to open. In order to modify the above result, in this case we require $\kappa_m = \sum_{j=1}^{3} \beta_{1j} a_j = 0$. Hence, Eq. (19a) is an identity. Taking into account that the opening of crack is attributed to application of electric loading for this case, we therefore use Eq. (19b) instead of Eq. (19a) to obtain dual integral equations similar to (36). An analogous treatment gives a solution as

$$A(\xi) = \frac{aJ_1(\xi a)}{\xi}\,\frac{\left[D_z^\infty - D^{(c)}\right]}{\kappa_e}, \tag{39}$$

where

$$\kappa_e = \sum_{j=1}^{3} \beta_{4j} a_j. \tag{40}$$

In view of (25c), it is readily seen that in the presence of mechanical loading, the solution (38) coincides with (39). Likely, (39) is valid only for $D_z^\infty \neq D^{(c)}$. For convenience, we rewrite these two results in a uniform form, i.e.

$$A(\xi) = \frac{aJ_1(\xi a)}{\xi}\,\frac{P}{\kappa}, \tag{41}$$

where

$$P = \sigma_0^\infty, \quad \kappa = \kappa_m, \quad \text{as } \sigma_0^\infty \neq 0, \tag{42}$$

$$P = D_z^\infty - D^{(c)}, \quad \kappa = \kappa_e, \quad \text{as } \sigma_0^\infty = 0. \tag{43}$$

With the above obtained results, a full electroelastic field in the entire piezoelectric plane with a dielectric crack can be determined. This can be achieved by substituting (41) into (13) for elastic displacements and potential. Making use of some equalities involving infinite integrals of Bessel functions (Fabrikant, 2003), explicit expressions for the elastic displacements and potential are obtained as follows:

$$u_x(x,z) = \frac{P}{\kappa}\sum_{j=1}^{3} a_j\left[x - \sqrt{x^2 - l_{1j}^2(x,z)}\right] + B_1 x, \tag{44a}$$

$$u_z(x,z) = \frac{P}{\kappa}\sum_{j=1}^{3} \eta_{3j}\gamma_j a_j\left[\sqrt{l_{2j}^2(x,z) - x^2} - \gamma_j z\right] + B_3 z, \tag{44b}$$

$$\phi(x,z) = \frac{P}{\kappa}\sum_{j=1}^{3} \eta_{4j}\gamma_j a_j\left[\sqrt{l_{2j}^2(x,z) - x^2} - \gamma_j z\right] + B_4 z, \tag{44c}$$

where some known integral identities have been utilized, which, together with B_k ($k = 1, 3, 4$) appearing in the above expressions, are given in Appendix A, and

$$l_{1j}(x,z) = \frac{1}{2}\left[\sqrt{(a+x)^2 + (\gamma_j z)^2} - \sqrt{(a-x)^2 + (\gamma_j z)^2}\right], \tag{45a}$$

$$l_{2j}(x,z) = \frac{1}{2}\left[\sqrt{(a+x)^2 + (\gamma_j z)^2} + \sqrt{(a-x)^2 + (\gamma_j z)^2}\right]. \tag{45b}$$

In a similar fashion, from (15), we can further give a complete solution of elastic stresses, strains, electric displacements, and electric fields in the entire plane. Or rather, the distribution of electroelastic field in the entire plane is

$$\sigma_{xx}(x,z) = \frac{P}{\kappa}\sum_{j=1}^{3} \beta_{0j} a_j\left[h_{2j}(x,z) - 1\right], \qquad \sigma_{zz}(x,z) = \frac{P}{\kappa}\sum_{j=1}^{3} \beta_{1j} a_j h_{2j}(x,z), \tag{46a}$$

$$\sigma_{xz}(x,z) = -\frac{P}{\kappa}\sum_{j=1}^{3} \beta_{2j} a_j h_{1j}(x,z), \tag{46b}$$

$$s_{xx}(x,z) = -\frac{P}{\kappa}\sum_{j=1}^{3} a_j\left[h_{2j}(x,z) - 1\right], \qquad s_{zz}(x,z) = \frac{P}{\kappa}\sum_{j=1}^{3} \eta_{3j}\gamma_j^2 a_j\left[h_{2j}(x,z) - 1\right], \tag{46c}$$

$$s_{xz}(x,z) = -\frac{P}{2\kappa}\sum_{j=1}^{3} \left(\eta_{3j} + 1\right)\gamma_j a_j h_{1j}(x,z), \tag{46d}$$

$$D_x(x,z) = -\frac{P}{\kappa}\sum_{j=1}^{3} \beta_{3j} a_j h_{1j}(x,z), \qquad D_z(x,z) = \frac{P}{\kappa}\sum_{j=1}^{3} \beta_{4j} a_j\left[h_{2j}(x,z) - 1\right] + D_z^{\infty}, \tag{46e}$$

$$E_x(x,z) = \frac{P}{\kappa}\sum_{j=1}^{3} \eta_{4j}\gamma_j a_j h_{1j}(x,z), \qquad E_z(x,z) = -\frac{P}{\kappa}\sum_{j=1}^{3} \eta_{4j}\gamma_j^2 a_j\left[h_{2j}(x,z) - 1\right], \tag{46f}$$

where

$$h_{1j}(x,z) = \frac{l_{1j}(x,z)\sqrt{a^2 - l_{1j}^2(x,z)}}{l_{2j}^2(x,z) - l_{1j}^2(x,z)}, \qquad h_{2j}(x,z) = \frac{l_{2j}(x,z)\sqrt{l_{2j}^2(x,z) - a^2}}{l_{2j}^2(x,z) - l_{1j}^2(x,z)}. \tag{47}$$

From the above, explicit analytic expressions for the entire electroelastic field are given through elementary functions. Generally speaking, γ_j's are probably related to complex numbers, but by a direct check one can find that all the quantities in the above-obtained electroelastic field are completely real. From a viewpoint, the derived solution is reasonable and correct. In reality, alternative expressions in terms of the real and imaginary parts of relevant complex functions involving $\sqrt{(x+\mathrm{i}\gamma_j z)^2-a^2}$ can also be given, which are omitted here. As indicated by Fabrikant (2003), it is very difficult to separate the corresponding real and imaginary parts into explicit expressions. However, the solution provided here is in simple, analytic, and explicit form.

On the other hand, if we confine our attention to the crack plane, we deduce immediately elastic displacements and potential, from the results (44), as

$$u_x(x,0)=\frac{P}{\kappa}\sum_{j=1}^{3}a_j\left[x-H(|x|-a)\sqrt{x^2-a^2}\right], \tag{48a}$$

$$u_z(x,0)=\frac{PH(a-|x|)}{\kappa}\sum_{j=1}^{3}\eta_{3j}\gamma_j a_j\sqrt{a^2-x^2}, \tag{48b}$$

$$\phi(x,0)=\frac{PH(a-|x|)}{\kappa}\sum_{j=1}^{3}\eta_{4j}\gamma_j a_j\sqrt{a^2-x^2}, \tag{48c}$$

and elastic stresses, electric displacement, and electric field, from the results (46), as

$$\sigma_{zz}(x,0)=\frac{\sigma_0^{\infty}|x|}{\sqrt{x^2-a^2}}H(|x|-a), \tag{49a}$$

$$\sigma_{xz}(x,0)=0, \tag{49b}$$

$$D_z(x,0)=\frac{\left[D_0^{\infty}-D^{(\mathrm{c})}\right]|x|}{\sqrt{x^2-a^2}}H(|x|-a)+D^{(\mathrm{c})}, \tag{49c}$$

$$E_z(x,0)=\left\{\frac{P}{\kappa}\sum_{j=1}^{3}\eta_{4j}\gamma_j^2 a_j\left[1-\frac{x}{\sqrt{x^2-a^2}}\right]+E_0^{\infty}\right\}H(|x|-a)+\frac{D^{(\mathrm{c})}}{\varepsilon^{(\mathrm{c})}}H(a-|x|), \tag{49d}$$

where $H(t)$ denotes the Heaviside unit step function, i.e. $H(t)=1$ for $t>0$ and $H(t)=0$ for $t<0$.

Obviously, $\sigma_{zz}(x,0)$ at the crack plane is independent of applied electric loading and material properties. Nevertheless, the distribution of $\sigma_{zz}(x,z)$ $(z\neq 0)$ around the crack tip is reliant on the material properties, which is apparently seen from (46a) owing to the dependence relation of κ_m and a_j on electric loading and the material properties. In contrast, in addition to applied electric loading and material properties, not only $D_z(x,z)$ $(z\neq 0)$ around the crack tip but also $D_z(x,0)$ at the crack plane depends upon applied mechanical loading, since the electric displacement $D^{(\mathrm{c})}$ at the crack surfaces is determined by electric loading as well as mechanical loading.

4. Fracture criterion

In studying the stability of a cracked piezoelectric structure, some facture criteria such as those of the maximum hoop stress and energy release rate in classical linear elastic fracture mechanics cannot be directly generalized to piezoelectric materials, since there exists a significant discrepancy between experimental

observations and theoretical predictions based on these criteria. In this section, MHS is suggested as a fracture criterion for piezoelectric materials, and the theoretical predictions based on this criterion agree closely with experimental data.

Fracture parameters are intimately relating to asymptotic field around the crack tip. Thus, prior to the presentation of this fracture criterion, it is expedient to determine asymptotic expressions for electroelastic field around the crack tip. For this purpose, we introduce a polar coordinate system (r,θ) with the origins at the right crack tip, as shown in Fig. 1, which satisfies

$$r=\sqrt{(x-a)^2+z^2},\qquad \theta=\tan^{-1}[z/(x-a)]. \tag{50}$$

In the close vicinity of the crack tip, i.e. $r\ll a$, we have

$$l_{1j}\simeq a+\frac{r}{2}\left[\cos(\theta)-\sqrt{\cos^2(\theta)+\gamma_j^2\sin^2(\theta)}\right], \tag{51a}$$

$$l_{2j}\simeq a+\frac{r}{2}\left[\cos(\theta)+\sqrt{\cos^2(\theta)+\gamma_j^2\sin^2(\theta)}\right]. \tag{51b}$$

Upon substitution of these into (46), by neglecting some higher-order infinitesimal terms, the asymptotic expressions for electroelastic field in the vicinity of the crack tip are derived below:

$$\begin{bmatrix}\sigma_{xx}(r,\theta)\\ \sigma_{zz}(r,\theta)\\ \sigma_{xz}(r,\theta)\end{bmatrix}\simeq\frac{P}{\kappa}\sqrt{\frac{a}{2r}}\sum_{j=1}^{3}\begin{bmatrix}\beta_{0j}a_jf_{2j}(\theta)\\ \beta_{1j}a_jf_{2j}(\theta)\\ -\beta_{2j}a_jf_{1j}(\theta)\end{bmatrix}+\mathrm{O}(1), \tag{52a}$$

$$\begin{bmatrix}s_{xx}(r,\theta)\\ s_{zz}(r,\theta)\\ s_{xz}(r,\theta)\end{bmatrix}\simeq\frac{P}{\kappa}\sqrt{\frac{a}{2r}}\sum_{j=1}^{3}\begin{bmatrix}-a_jf_{2j}(\theta)\\ \eta_{3j}\gamma_j^2a_jf_{2j}(\theta)\\ -(1+\eta_{3j})\gamma_ja_jf_{1j}(\theta)/2\end{bmatrix}+\mathrm{O}(1), \tag{52b}$$

$$\begin{bmatrix}D_x(r,\theta)\\ D_z(r,\theta)\\ E_x(r,\theta)\\ E_z(r,\theta)\end{bmatrix}\simeq\frac{P}{\kappa}\sqrt{\frac{a}{2r}}\sum_{j=1}^{3}\begin{bmatrix}-\beta_{3j}a_jf_{1j}(\theta)\\ \beta_{4j}a_jf_{2j}(\theta)\\ \eta_{4j}\gamma_ja_jf_{1j}(\theta)\\ -\eta_{4j}\gamma_j^2a_jf_{2j}(\theta)\end{bmatrix}+\mathrm{O}(1), \tag{52c}$$

where $f_{1j}(\theta)$ and $f_{2j}(\theta)$ denote the functions of angle distribution, defined by

$$f_{1j}(\theta)=\frac{1}{\sqrt[4]{\cos^2(\theta)+\gamma_j^2\sin^2(\theta)}}\sqrt{\frac{1}{2}\left[1-\frac{\cos(\theta)}{\sqrt{\cos^2(\theta)+\gamma_j^2\sin^2(\theta)}}\right]}, \tag{53a}$$

$$f_{2j}(\theta)=\frac{1}{\sqrt[4]{\cos^2(\theta)+\gamma_j^2\sin^2(\theta)}}\sqrt{\frac{1}{2}\left[1+\frac{\cos(\theta)}{\sqrt{\cos^2(\theta)+\gamma_j^2\sin^2(\theta)}}\right]}, \tag{53b}$$

which are universal and pertain to all crack configurations and loading conditions, but depend on the roots of the characteristic equation (11).

From the above, the intensity factors of stress, strain, electric-displacement and electric-field near the crack tip, according to their definitions

$$K^q = \lim_{x\to a^+} \sqrt{2\pi(x-a)}q(x,0), \tag{54}$$

where q stands for σ_{zz}, s_{zz}, D_z, and E_z, respectively, can be evaluated as

$$K^\sigma = \sigma_0^\infty\sqrt{\pi a}, \qquad K^s = \frac{P}{\kappa}\sum_{j=1}^{3}\eta_{3j}\gamma_j^2 a_j\sqrt{\pi a}, \tag{55a}$$

$$K^D = \left[D_z^\infty - D^{(c)}\right]\sqrt{\pi a}, \qquad K^E = -\frac{P}{\kappa}\sum_{j=1}^{3}\eta_{4j}\gamma_j^2 a_j\sqrt{\pi a}. \tag{55b}$$

As a by-production, another important fracture parameter, the elastic T-stress, defined as the nonsingular term of asymptotic field σ_{xx} near the crack tip and is used to characterize constraint around the crack tip, is found from (46a) to be

$$T = -\frac{P}{\kappa}\sum_{j=1}^{3}\beta_{0j}a_j. \tag{56}$$

Clearly the elastic T-stress is dependent on applied electric loading and the material properties, while K^σ is independent of applied electric loading and the material properties. No matter how applied electric loading varies, stress intensity factor maintains unchanged, implying that stress intensity factors near the crack tip is inapplicable to predicting crack growth of piezoelectric materials.

On the other hand, for a piezoelectric material, the total energy release rate, defined as the released energy per unit length during crack growth under combined electromechanical loading, consists of two parts: $G = G^{\mathrm{m}} + G^{\mathrm{e}}$, G^{m} and G^{e} are so-called mechanical strain energy release rate and electric energy release rate, which can respectively be evaluated by the following integrals ($0 < \delta \ll a$):

$$G^{\mathrm{m}} = \lim_{\delta\to 0}\frac{1}{2\delta}\int_0^\delta \sigma_{zz}(r,0)[u_z(\delta-r,\pi) - u_z(\delta-r,-\pi)]\,\mathrm{d}r, \tag{57}$$

$$G^{\mathrm{e}} = \lim_{\delta\to 0}\frac{1}{2\delta}\int_0^\delta D_z(r,0)[\phi(\delta-r,\pi) - \phi(\delta-r,-\pi)]\,\mathrm{d}r, \tag{58}$$

where u_z is also influenced by applied electric field because of the coupling characteristic, and aside from electric loading, ϕ is also related to mechanical loading. Substituting asymptotic expressions for the stress and displacement into the above integrals yields

$$G^{\mathrm{m}} = \frac{\pi a\sigma_{zz}^\infty}{2}\frac{P}{\kappa}\sum_{j=1}^{3}\eta_{3j}\gamma_j a_j, \qquad G^{\mathrm{e}} = \frac{\pi a\left[D_z^\infty - D^{(c)}\right]}{2}\frac{P}{\kappa}\sum_{j=1}^{3}\eta_{4j}\gamma_j a_j, \tag{59}$$

where P and κ are defined as before. The total energy release rate G is therefore given by

$$G = \frac{\pi a P}{2\kappa}\left[\sigma_{zz}^\infty\sum_{j=1}^{3}\eta_{3j}\gamma_j a_j + \left(D_z^\infty - D^{(c)}\right)\sum_{j=1}^{3}\eta_{4j}\gamma_j a_j\right] \tag{60}$$

or

$$G = \frac{\pi a}{2}\frac{P}{\kappa}\sum_{j=1}^{3}\left[\sigma_{zz}^\infty - \frac{1}{\varepsilon^{(c)}}D^{(c)}\left(D_z^\infty - D^{(c)}\right)\right]\eta_{3j}\gamma_j a_j \tag{61}$$

in view of (25b). Especially, for an impermeable crack, $\varepsilon^{(c)} = 0$, and $D^{(c)} = 0$; so the above result reduces to

$$G = \frac{\pi a}{2}\sum_{j=1}^{3}\left[\frac{(\sigma_{zz}^{\infty})^2}{\kappa_m}\eta_{3j}\gamma_j a_j + \frac{(D_z^{\infty})^2}{\kappa_e}\eta_{4j}\gamma_j a_j\right]. \tag{62}$$

Computational results indicate that, similar to that for an impermeable crack, G^{e} for a dielectric crack is also always negative regardless of positive or negative electric fields, inferring that any electric field impedes crack growth for piezoelectric materials, contrary to experimental results. If adopting the viewpoint that G^{e} is responsible for the breakdown of electric behavior in dielectrics (Garboczi, 1988; Ouyang and Lee, 1998) and G^{m} for the failure of mechanical behavior (Park and Sun, 1995; Guiu et al., 2003), we neglect G^{e} and have $G = G^{\mathrm{m}}$. Furthermore, $G^{\mathrm{m}} = 0$ in the absence of mechanical loading, which is inconsistency with experimental findings that purely electric fields can also drive crack propagation in a poled ferroelectric ceramic (Cao and Evans, 1994; Schneider and Heyer, 1999; Shang and Tan, 2001; dos Santos e Lucato et al., 2002).

In the present paper, the MHS criterion (Ayari and Ye, 1995; Chang, 1981) is suggested as a fracture criterion. A basic reason is that a crack can advance ahead only because of the result of crack deformation, which can be generated by not only mechanical loading but also electric loading. Since the MHS in the close vicinity of the crack tip ($r \ll a$) can be characterized by the strain intensity factor K^s, the MHS criterion, in effect, is equivalent to the strain intensity factor criterion. It follows from the second in (55a) that K^s is apparently dependent on mechanical loading as well as electric loading, implying that crack growth can be driven by both mechanical loading and electric loading, even by purely electric fields. Similar to the hypotheses for the maximum hoop stress criterion, for the MHS criterion the following hypotheses are adopted (Ayari and Ye, 1995; Chang, 1981).

Hypothesis 1. Crack initiation starts when the maximum of the hoop strain $s_{\theta\theta}$ reaches a critical value, which is a material constant.

Hypothesis 2. Crack initiation is assumed to occur in the direction along which $s_{\theta\theta}$ arrives at a maximum.

5. Numerical results and discussions

To demonstrate the effectiveness of the MHS criterion as a fracture criterion of piezoelectric materials, in this section, as a numerical example we consider a commercially available PZT-4 ceramic and study the influence of applied electric field on crack growth through the MHS criterion. When a PZT-4 is poled along the z-axis, it exhibits transversely isotropic behavior and the relevant material properties are given in Table 1 (Park and Sun, 1995). Here of interest is the case where a plane crack perpendicular to the poling axis penetrates through the PZT-4 ceramic along the y-axis.

In order to determine the direction of crack initiation, the angle distribution of the hoop strain, normalized by multiplying $s_{\theta\theta}(r,\theta)$ by $\sqrt{2r/a}$, around the crack tip is plotted for a vacuum dielectric-crack with different applied electric fields in the presence and absence of mechanical loading in Figs. 4 and 5, respectively. It is readily found from Fig. 4 that the MHS $s_{\theta\theta}$ occurs at $\theta = 0°$, indicating that crack propagates along the crack plane and cannot branch or deflect for any combined electromechanical loading, which agrees with the experimental observations by Park and Sun (1995) and with the theoretical predictions through the finite element method according to the energy release rate criterion (Kumar and Singh, 1998). Also, the MHS becomes larger for a positive electric field, or less for a negative electric field than that in purely mechanical loading, inferring that positive electric fields promote crack growth and negative ones hinder crack growth, coinciding qualitatively with experiment findings of Park and Sun (1995). Moreover, irrespective of the sign of applied electric fields, the strain in front of the crack tip $s_{\theta\theta}$ is

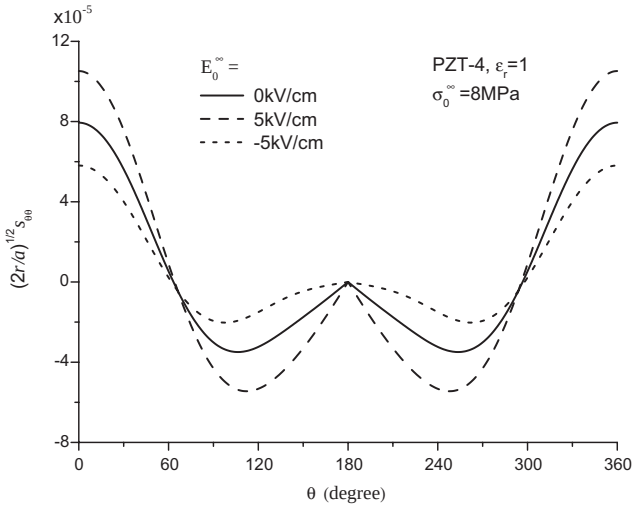

Fig. 4. Angle distribution of the hoop strain with $\sigma_0^{\infty} = 8$ MPa for a PZT ceramic containing a vacuum crack.

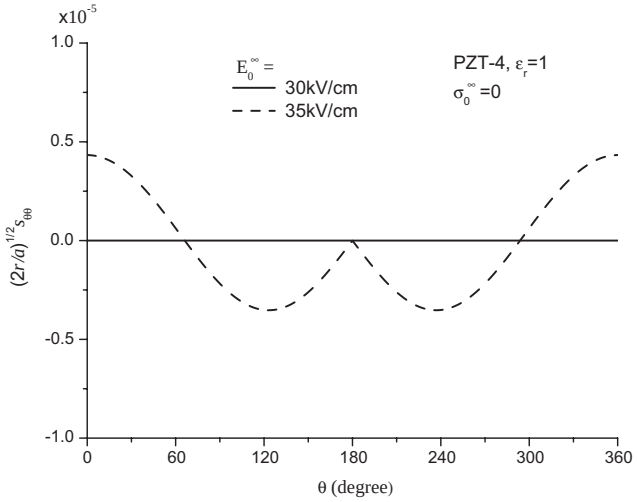

Fig. 5. Angle distribution of the hoop strain with $\sigma_0^{\infty} = 0$ for a PZT ceramic containing a vacuum crack.

tensile in a range of $|\theta| < 62°$, 63°, and 64° for $E_0^{\infty} = -5$, 0, and 5 kV/cm, respectively, and is compressive in other regions, causing the crack to open and even to propagate along the crack plane. In contrast, from (49a) the maximum hoop stress $\sigma_{\theta\theta}$ at $\theta = 0$ is not reliant on applied electric fields, although the maximum hoop stress $\sigma_{\theta\theta}$ also takes place at $\theta = 0$ and $\sigma_{\theta\theta}$ when $\theta \neq 0$ depends slightly on electric fields, which indicates that crack initiation is controlled by the MHS rather than the maximum hoop stress. It is worth noting that in the previous study (Pak, 1992; Sosa, 1992; Kumar and Singh, 1996), enough high negative electric fields may cause a crack to deviate from the original crack plane in crack growth for an impermeable crack. However, the present study indicates that this case seems not to take place, since negative electric fields cause crack opening to decrease and even to close, and in this case the electric displacement at the crack surfaces are a nonvanishing constant rather than zero due to the perfect contact of two crack

surfaces. In fact, according to the energy release rate criterion, a crack indeed propagates in a straight line along the crack plane for any combined electromechanical loading (Kumar and Singh, 1998), identical to that according to the MHS criterion. Furthermore, in the absence of mechanical loading (Fig. 5), purely electric fields, if it rises high enough, may drive crack propagation.

Dependence of the MHS on applied electric fields is given in the presence and absence of mechanical loading, $\sigma_0^\infty = 8$ MPa, and 0, for different dielectric permittivities of the crack interior in Figs. 6(a) and 7(a), respectively. For comparison, in Figs. 6(b) and 7(b), the normalized crack center opening displacement, $u_z(0,0)/a$, is presented for the corresponding cases, since $u_z(0,0)/a$ is also a significant fracture parameter accounting for crack opening. From these figures we find that both the MHS and the normalized crack center opening displacement remain unchanged for a conducting crack, which depend only upon applied mechanical loading and not only electric fields. This is an obvious conclusion for a conducting crack. As expected, purely electric fields fail to generate any MHS and crack opening displacement for a conducting

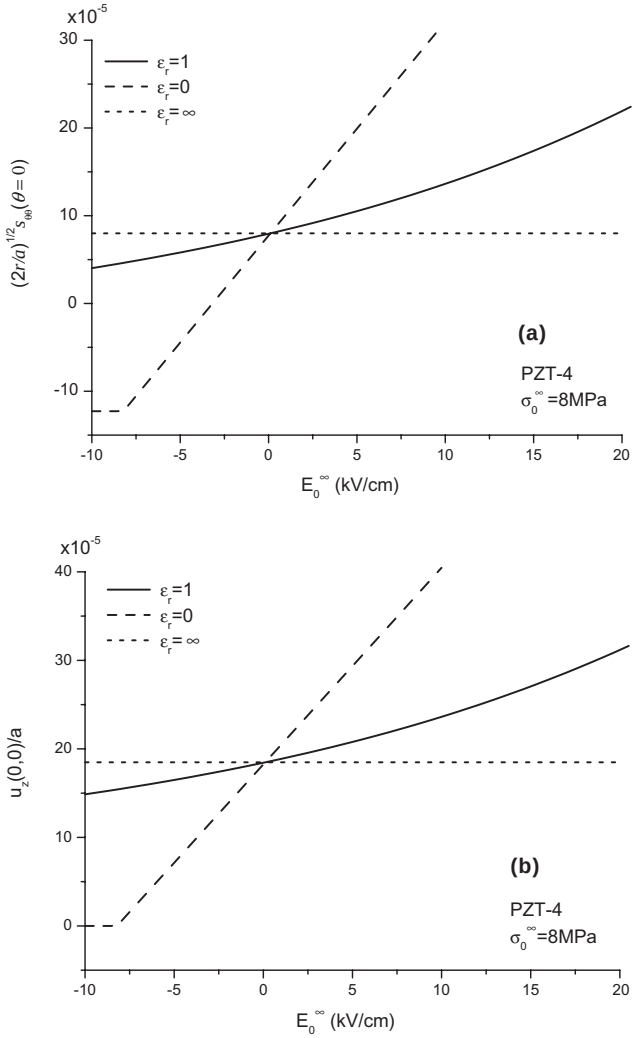

Fig. 6. (a) MHS and (b) crack center opening displacement versus applied electric field with $\sigma_0^\infty = 8$ MPa for a cracked PZT.

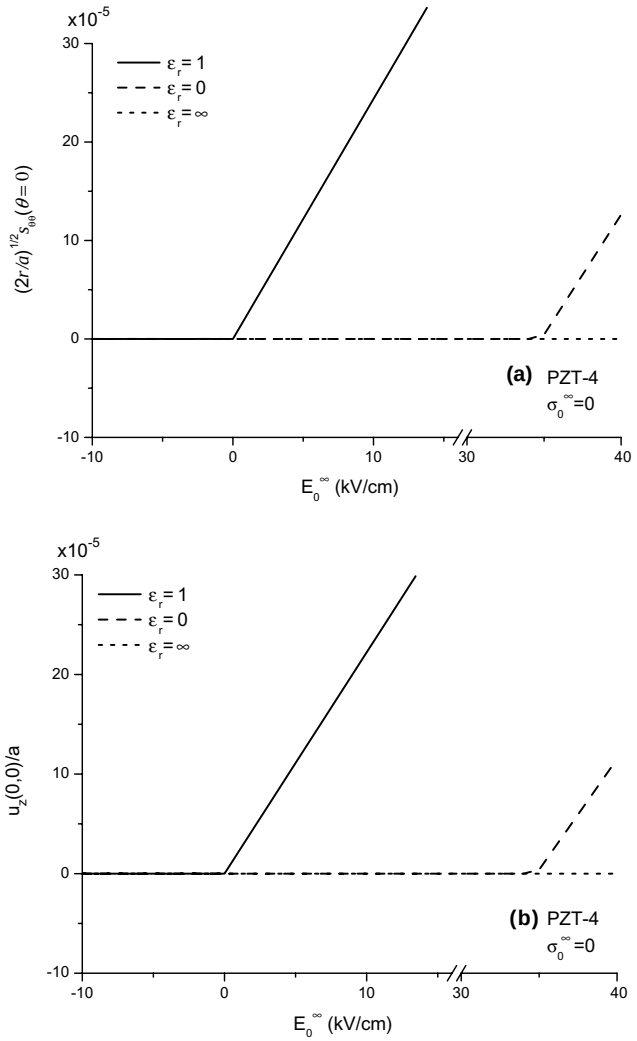

Fig. 7. (a) MHS and (b) crack center opening displacement versus applied electric field with $\sigma_0^{\infty} = 0$ for a cracked PZT.

crack. However, for an impermeable crack with the relative dielectric constant $\varepsilon_r = 0$ of the crack interior, the MHS ahead of the crack tip has a plateau and exhibits constant compressive behavior in a range of lower applied electric fields. From Fig. 6(b) we find that at this stage, there is no crack opening displacement. In other words, under such combined electromechanical loading, crack does not open and maintains closed for an enough high negative electric field, which can be explained by the fact that a negative electric field cause a piezoelectric material to shrink in the poling axis. And when applied electric fields exceed a certain (negative) value, the MHS as well as the crack center opening displacement rises in a straight line as electric field is raised. For a real vacuum crack with $\varepsilon_r = 1$, a plateau similar to those for an impermeable crack has not been found when electric field lies in the interval $[-10, 20]$. Moreover, the MHS is always tensile and the crack is always open in the presence of mechanical loading $\sigma_0^{\infty} = 8$ MPa, although applied negative electric fields decrease the MHS as well as the crack center opening displacement. It is also observed from Fig. 6(a) that the MHS is increased with increasing applied electric field for a vacuum

dielectric-crack, which again implies the consistency with experimental results. And the same trend is visible for the crack center opening displacement in Fig. 6(b).

In the absence of mechanical loading, from Fig. 7 it is seen that any purely electric fields fail to drive a conducting crack to open, which is as expected. For an impermeable crack with $\varepsilon_r = 0$, a crack immediately opens provided that positive electric fields are applied, and maintains closed provided that negative electric fields are applied. However, for a vacuum crack with $\varepsilon_r = 1$, the turning point of applied electric field from a closed crack to a open crack is shifted from zero to a higher positive electric field, which is clearly due to the influence of the dielectric permittivity of the crack interior on crack growth. From the above, for a nonconducting crack, an important conclusion can be drawn out. That is, purely electric fields can also drive fatigue crack growth, which may explain crack growth driven by purely electric fields observed in a poled ferroelectric ceramic in experiment (Cao and Evans, 1994; Schneider and Heyer, 1999; Shang and Tan, 2001). It is noted that this phenomenon cannot be predicted according to the fracture criterion of the mechanical strain energy release rate (Park and Sun, 1995), since it vanishes in the absence of mechanical loading.

Finally, based on the MHS criterion proposed in the present paper, a comparison between the theoretical predictions and the experimental results of Park and Sun (1995) is made. The experimental setup of a compact tension specimen adopted by Park and Sun is depicted in Fig. 8. Applied electric field E was

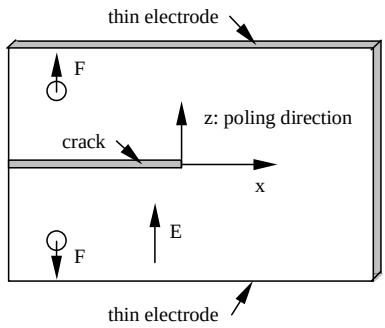

Fig. 8. Schematic diagram of a compact tension specimen subjected to electromechanical loadings.

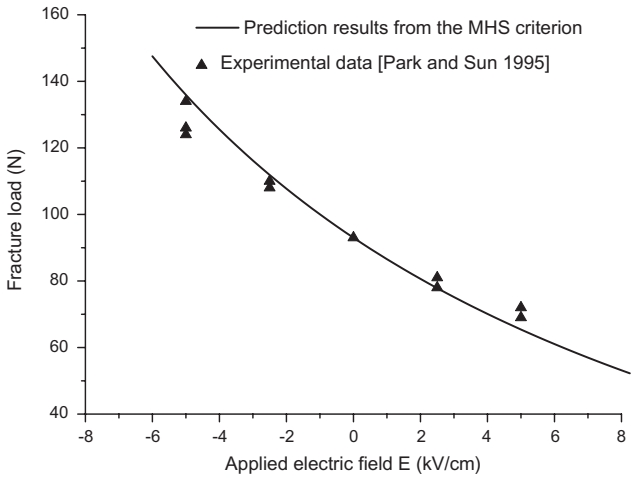

Fig. 9. Comparison of theoretical predictions and experimental measures for PZT-4 ceramic.

generated by controlling a voltage between two opposite top and bottom surface thin electrodes. Under a certain electric field, mechanical tensive loading was applied, and the procedure of testing was to increase the tensive load until fracture occurred.

From the experimental data of Park and Sun (1995), the fracture initiation loads F under different electric fields are shown in Fig. 9. Especially, in the absence of applied electric field, the fracture load F is estimated about 93 N, from which we derive a critical value of the MHS. In what follows we start with this critical value. According to the MHS criterion, the relation between the fracture loads F and applied electric fields E_0^∞ should be lie at a certain contour line of $s_{\theta\theta}$ equal to the critical value, which is displayed in Fig. 9. From Fig. 9, it is readily seen that the theoretical predictions in the presence of applied electric field give the fracture loads $F = 136$, 111, 78, 66 N corresponding to $E_0^\infty = -5$, -2.5, 2.5, 5 kV/cm, respectively, in satisfactory agreement with the experimental measures given by Park and Sun (1995). This indicates that the MHS criterion is a potential fracture criterion for piezoelectric materials. Of course, it is worth noting that like other fracture criteria, the MHS criterion is also a macroscopic one which does not reflect the mesomechanical and micromechanical behaviors of piezoelectric materials.

6. Conclusions

In addition to mechanical stress, purely electric loading also produce deformation due to the coupling feature between elastic and electric behaviors of piezoelectric materials. Crack opening is only due to the direct results of crack deformation, and crack growth is therefore attributed not only to mechanical stress but also to electric loading. Based on this assumption, the MHS is suggested as a fracture criterion of piezoelectric materials. Using this criterion, relevant experimental results can be successfully explained, that is, applied electric fields can enhance and hinder crack propagation, depending on positive and negative electric fields. Furthermore, purely electric field may also drive crack growth, regardless of the presence of applied mechanical loading. Some main conclusions are summarized as follows.

- The MHS is suggested as an effective facture criterion. The theoretical predictions are in excellent agreement with experimental data.
- The electric displacement at the crack surfaces depends nonlinearly upon applied electromechanical loading for a dielectric crack. A linear approximation of the electric displacement at the crack surface on applied electric field is present and exhibits a satisfactory accuracy.
- The complete electroelastic field for a dielectric crack is obtained in terms of elementary functions, and the asymptotic crack-tip field is also determined in terms of two unified angle distribution functions. Impermeable and conducting cracks are special cases of dielectric crack as the dielectric permittivity of the crack interior vanishes and approaches infinity, respectively.

Acknowledgements

This work was supported by the National Natural Science Foundation of China under Grant No. 10272043 and the Korea Institute of Science and Technology Evaluation and Planning.

Appendix A

The constants appearing in the characteristic equation (11) are

$$a_0 = c_{44}\left(c_{33}\varepsilon_{33} + e_{33}^2\right), \tag{A.1}$$

$$b_0 = -2c_{44}e_{15}e_{33} - c_{11}e_{33}^2 - c_{33}(c_{44}\varepsilon_{11} + c_{11}\varepsilon_{33}) + \varepsilon_{33}(c_{13} + c_{44})^2 + 2e_{33}(c_{13} + c_{44})(e_{31} + e_{15}) - c_{44}^2\varepsilon_{33} - c_{33}(e_{31} + e_{15})^2, \tag{A.2}$$

$$c_0 = 2c_{11}e_{15}e_{33} + c_{44}e_{15}^2 + c_{11}(c_{33}\varepsilon_{11} + c_{44}\varepsilon_{33}) - \varepsilon_{11}(c_{13} + c_{44})^2 - 2e_{15}(c_{13} + c_{44})(e_{31} + e_{15}) + c_{44}^2\varepsilon_{11} + c_{44}(e_{31} + e_{15})^2, \tag{A.3}$$

$$d_0 = -c_{11}\left(c_{44}\varepsilon_{11} + e_{15}^2\right). \tag{A.4}$$

By solving the resulting equations, the unknown constants B_k, $(k = 1, 3, 4)$ are obtained as

$$B_1 = \frac{-c_{13}\sigma_0^\infty + (c_{33}e_{31} - c_{13}e_{33})E_0^\infty}{c_{11}c_{33} - c_{13}^2}, \tag{A.5}$$

$$B_3 = \frac{c_{11}\sigma_0^\infty + (c_{11}e_{33} - c_{13}e_{31})E_0^\infty}{c_{11}c_{33} - c_{13}^2}, \tag{A.6}$$

$$B_4 = -E_0^\infty, \tag{A.7}$$

In Eq. (32), the coefficients m_0, m_1, and m_2 are, respectively,

$$m_0 = \varepsilon^{(c)}\sigma_0^\infty \det[\beta_4, \beta_2, \eta_2] - \varepsilon^{(c)}D_z^\infty \det[\beta_1, \beta_2, \eta_2], \tag{A.8}$$

$$m_1 = \varepsilon^{(c)} \det[\beta_1, \beta_2, \eta_2] + \sigma_0^\infty \det[\beta_4, \beta_2, \eta_1] - D_z^\infty \det[\beta_1, \beta_2, \eta_1], \tag{A.9}$$

$$m_2 = \det[\beta_1, \beta_2, \eta_1]. \tag{A.10}$$

In deriving (44) and (46), the following integral identities:

$$\int_0^\infty \frac{1}{\xi} e^{-c\xi} J_1(a\xi)\cos(b\xi)\,d\xi = \frac{1}{a}\left[\sqrt{l_2^2 - b^2} - c\right], \tag{A.11}$$

$$\int_0^\infty \frac{1}{\xi} e^{-c\xi} J_1(a\xi)\sin(b\xi)\,d\xi = \frac{1}{a}\left[b - \sqrt{b^2 - l_1^2}\right], \tag{A.12}$$

$$\int_0^\infty e^{-c\xi} J_1(a\xi)\cos(b\xi)\,d\xi = \frac{1}{a} - \frac{l_2}{a}\frac{\sqrt{l_2^2 - a^2}}{l_2^2 - l_1^2}, \tag{A.13}$$

$$\int_0^\infty e^{-c\xi} J_1(a\xi)\sin(b\xi)\,d\xi = \frac{l_1}{a}\frac{\sqrt{a^2 - l_1^2}}{l_2^2 - l_1^2}, \tag{A.14}$$

have been utilized, which can be readily shown from Fabrikant (2003), where $\mathrm{Re}(c) > |\mathrm{Im}(a \pm b)|$,

$$l_1 = \frac{1}{2}\left[\sqrt{(a+b)^2 + c^2} - \sqrt{(a-b)^2 + c^2}\right], \tag{A.15}$$

$$l_2 = \frac{1}{2}\left[\sqrt{(a+b)^2 + c^2} + \sqrt{(a-b)^2 + c^2}\right]. \tag{A.16}$$

References

Ayari, M.L., Ye, Z., 1995. Maximum strain theory for mixed mode crack propagation in anisotropic solids. Eng. Fract. Mech. 52, 389–400.

Cao, H., Evans, A.G., 1994. Electric-field-induced fatigue crack growth in piezoelectrics. J. Am. Ceram. Soc. 77, 1783–1786.

Chang, K.J., 1981. On the maximum strain criterion—a new approach to the angled crack problem. Eng. Fract. Mech. 14, 107–124.

dos Santos e Lucato, S.L., Bahr, H.-A., Pham, V.-B., Lupascu, D.C., Balke, H., Rodel, J., Bahr, U., 2002. Electrically driven cracks in piezoelectric ceramics: experiments and fracture mechanics analysis. J. Mech. Phys. Solids 50, 2333–2353.

Dunn, M.L., 1994. The effects of crack face boundary conditions on the fracture mechanics of piezoelectric solids. Eng. Fract. Mech. 48, 25–39.

Fabrikant, V.I., 2003. Computation of infinite integrals involving three Bessel functions by introduction of new formalism. ZAMM 83, 363–374.

Fang, D.N., Liu, B., Hwang, K.C., 1999. Energy analysis on fracture of ferroelectric ceramics. Int. J. Fract. 100, 401–408.

Fulton, C.C., Gao, H., 2001. Effect of local polarization switching on piezoelectric fracture. J. Mech. Phys. Solids 49, 927–952.

Gao, C.-F., Fan, W.X., 1999. Exact solutions for the plane problem in piezoelectric materials with an elliptic or a crack. Int. J. Solids Struct. 36, 2527–2540.

Gao, H., Zhang, T.-Y., Tong, P., 1997. Local and global energy release rates for an electrically yielded crack in a piezoelectric ceramic. J. Mech. Phys. Solids 45, 491–510.

Garboczi, E.J., 1988. Linear dielectric-breakdown electrostatics. Phys. Rev. B. 38, 9005–9010.

Guiu, F., Alguero, M., Reece, M.J., 2003. Crack extension force and rate of mechanical work of fracture in linear dielectrics and piezoelectrics. Phil. Mag. 83, 873–888.

Hao, T.H., Shen, Z.Y., 1994. A new electric boundary condition of electric fracture mechanics and its applications. Eng. Fract. Mech. 47, 793–802.

Hwang, S.C., Lynch, C.S., McMeeking, R.M., 1995. Ferroelectric/ferroelastic interactions and polarization switch model. Acta Metall. Mater. 43, 2073–2084.

Kumar, S., Singh, R.N., 1996. Crack propagation in piezoelectric materials under combined mechanical and electrical loadings. Acta Mater. 44, 173–200.

Kumar, S., Singh, R.N., 1998. Effect of the mechanical boundary condition at the crack surfaces on the stress distribution at the crack tip in piezoelectric materials. Mater. Sci. Eng. A 252, 64–77.

Liu, M., Hsia, K.J., 2003. Interfacial cracks between piezoelectric and elastic materials under in-plane electric loading. J. Mech. Phys. Solids 51, 921–944.

Liu, B., Fang, D.-N., Soh, A.K., Hwang, K.-C., 2001. An approach for analysis of poled/depolarized piezoelectric materials with a crack. Int. J. Fract. 111, 395–407.

McMeeking, R.M., 1999. Crack tip energy release rate for a piezoelectric compact tension specimen. Eng. Fract. Mech. 64, 217–244.

McMeeking, R.M., 2001. Towards a fracture mechanics for brittle piezoelectric and dielectric materials. Int. J. Fract. 108, 25–41.

Ouyang, H., Lee, S., 1998. Application of linear elastic fracture mechanics on electric discharge breakdown in interconnects. Appl. Phys. Lett. 73, 3565–3567.

Pak, Y.E., 1990. Crack extension force in a piezoelectric material. J. Appl. Mech. 57, 647–653.

Pak, Y.E., 1992. Linear electro-elastic fracture mechanics of piezoelectric materials. Int. J. Fract. 54, 79–100.

Park, S., Sun, C.T., 1995. Fracture criteria for piezoelectric ceramics. J. Am. Ceram. Soc. 78, 1475–1480.

Pisarenko, G.G., Chushko, V.M., Kovalev, S.P., 1985. Anisotropy of fracture toughness in piezoelectric ceramics. J. Am. Ceram. Soc. 68, 259–265.

Rajapakse, R.K.N.D., 1997. Plane strain/stress solutions for piezoelectric solids. Compos. Part. B. 28, 385–396.

Rao, S.S., Sunar, M., 1994. Piezoelectricity and its use in disturbance sensing and control of flexible structures: a survey. Appl. Mech. Rev. 47, 113–123.

Ru, C.Q., 1999. Electric-field induced crack closure in linear piezoelectric media. Acta Mater. 47, 4683–4693.

Schneider, G.A., Heyer, V., 1999. Influence of the electric field on Vickers indentation crack growth in $BaTiO_3$. J. Euro. Ceram. Soc. 19, 1299–1306.

Schneider, G.A., Felten, F., McMeeking, R.M., 2003. The electrical potential difference across cracks in PZT measured by Kelvin Probe Microscopy and the implications for fracture. Acta Mater. 51, 2235–2241.

Shang, J.K., Tan, X., 2001. A maximum strain criterion for electric-field-induced fatigue crack propagation in ferroelectric ceramics. Mater. Sci. Eng. A 301, 131–139.

Shindo, Y., Tanaka, K., Narita, F., 1997. Singular stress and electric fields of a piezoelectric ceramic strip with a finite crack under longitudinal shear. Acta Mech. 120, 31–45.

Shindo, Y., Watanabe, K., Narita, F., 2000. Electroelastic analysis of a piezoelectric ceramic strip with a central crack. Int. J. Eng. Sci. 38, 1–19.

Sosa, H., 1992. On the fracture mechanics of piezoelectric solids. Int. J. Solids Struct. 29, 2613–2622.

Sosa, H., Khutoryansky, N., 1996. New developments concerning piezoelectric materials with defects. Int. J. Solids Struct. 33, 3399–3414.

Suo, Z., Kuo, C.-M., Barnett, D.M., Willis, J.R., 1992. Fracture mechanics for piezoelectric ceramics. J. Mech. Phys. Solids 40, 739–765.

Tobin, A.G., Pak, Y.E., 1993. Effect of electric fields on the fracture behaviour of PZT ceramics. Proc. SPIE 1916/79, 78–86.

Wang, X.D., Jiang, L.Y., 2002. Fracture behaviour of cracks in piezoelectric media with electromechanically coupled boundary conditions. Proc. R. Soc. Lond. A 458, 2545–2560.

Wang, B.L., Mai, Y.-W., 2003. On the electrical boundary conditions on the crack surfaces in piezoelectric ceramics. Int. J. Eng. Sci. 41, 633–652.

Xu, X.-L., Rajapakse, R.K.N.D., 2001. On a plane crack in piezoelectric solids. Int. J. Solids Struct. 38, 7643–7658.

Yang, F., 2001. Fracture mechanics for a Mode I crack in piezoelectric materials. Int. J. Solids Struct. 38, 3813–3830.

Yang, W., Zhu, T., 1998. Switch-toughnessing of ferroelectrics subjected to electric fields. J. Mech. Phys. Solids 46, 291–311.

Zhang, T.-Y., Qian, C.-F., Tong, P., 1998. Linear electro-elastic analysis of a cavity or a crack in a piezoelectric material. Int. J. Solids Struct. 35, 2121–2149.